Theoretical study of the O-H stretching band in 3-hydroxy-2-methyl-4-pyrone

V. Alexandrov, D. M. A. Smith, H. Rostkowska, M. J. Nowak, L. Adamowicz, and W. McCarthy

Citation: The Journal of Chemical Physics **108**, 9685 (1998); doi: 10.1063/1.476444
View online: http://dx.doi.org/10.1063/1.476444
View Table of Contents: http://scitation.aip.org/content/aip/journal/jcp/108/23?ver=pdfcov
Published by the AIP Publishing

Theoretical study of the O-H stretching band in 3-hydroxy-2-methyl-4-pyrone

V. Alexandrov and D. M. A. Smith
Department of Chemistry, University of Arizona, Tucson, Arizona 85721

H. Rostkowska and M. J. Nowak
Institute of Physics, Polish Academy of Science, Warsaw, Poland

L. Adamowicz
Department of Chemistry, University of Arizona, Tucson, Arizona 85721

W. McCarthy
Biotechnology Center, Utah State University, Logan, Utah 84322-470521

(Received 6 November 1997; accepted 11 March 1998)

The infrared spectrum of 3-hydroxy-2-methyl-4-pyrone reveals an O-H stretching frequency roughly 200 cm^{-1} lower than that of a typical alcohol group. The frequency lowering results from intramolecular hydrogen bonding between the alcohol and ketone groups. In this work, the stretching and bending vibrations of the O-H group in 3-hydroxy-2-methyl-4-pyrone are studied with a theoretical methodology more rigorous than the conventional harmonic approximation. A two-dimensional potential energy surface in internal coordinates corresponding to different hydrogen positions in the plane of the molecule is calculated with the use of the second order Møller-Plesset perturbation theory. To include all possible variations in kinetic energy in a large amplitude vibrational mode, g-matrix elements with variable values are employed. The analytical expression for the Hamiltonian matrix elements of the two-dimensional vibrational problem in a basis of shifted Gaussian functions is derived. Expectation values for the O-H stretch nuclear states are variationally determined with the use of shifted Gaussian functions as the basis set. The results of the calculations are compared with the recent matrix-isolation infrared (IR) spectroscopic results. The calculated transition frequency corresponding to the in-plane O-H stretching is found to be in good agreement with the experimental value. © *1998 American Institute of Physics.* [S0021-9606(98)00923-4]

I. INTRODUCTION

Infrared spectroscopy is an indispensable tool for determining molecular structure. This technique is almost exclusively applied in structural studies of transient compounds, or compounds existing in interstellar clouds.[1,2] The identification of the structure becomes trivial if the compound of interest has already been ''fingerprinted;'' however, when ''new'' compounds are encountered a more involved procedure leading to the determination of the structure of the molecule must be utilized. One such procedure is based on comparison between the IR spectra obtained experimentally and the spectra simulated theoretically. This combined experimental-theoretical technique consists of comparison of the experimental IR spectra to *ab initio* calculated harmonic frequencies scaled by an appropriate factor.[3–8] The scaling factor is an empirically derived quantity intended to compensate for the inherent shortcomings of the theoretical method applied, such as an incomplete basis set, neglect of some electron correlation, and lack of anharmonicity. The IR spectra of matrix-isolated nucleic acid bases and their analogs are routinely interpreted with a combined matrix-isolation theoretical method.[9–11] Simulated spectra are most readily compared with gas-phase, or matrix-isolated, experimental IR spectra where intermolecular interactions are nonexistent, or minimal. However, there have been several IR spectra of matrix-isolated hydrogen-bonded complexes which have been successfully assigned by comparison to scaled *ab initio* harmonic frequencies.[3–8,12] The most difficult frequencies to assign in these comparisons have been vibrational modes involving motion of the H-bonded atoms.

The molecule 3-hydroxy-2-methyl-4-pyrone, also known as maltol, is present in red Korean ginseng, and is used as a food flavoring.[13–20] There exists in the molecule an intramolecular hydrogen bond between the alcohol and ketone groups (see Fig. 1). The intramolecular hydrogen bond causes a lowering of the vibrational frequency of the O-H stretch; the experimental value for the O-H stretch, which typically occurs between 3550 and 3600 cm^{-1} for alcohols, was found to be 3381 cm^{-1} in 3-hydroxy-2-methyl-4-pyrone (see Fig. 2). Beyond being an analog of pyrimidine derivative nucleic acid bases, 3-hydroxy-2-methyl-4-pyrone also provides a convenient model for studying vibrational frequency shifts caused by hydrogen bonding. The best and simplest description of vibrational motion in 3-hydroxy-2-methyl-4-pyrone is given within an internal coordinate system. Internal coordinates directly reflect the structure of the molecule, and provide the most concise description of potential energy. There are many vibrational modes which can be described by only a small subset of the internal coordinates;

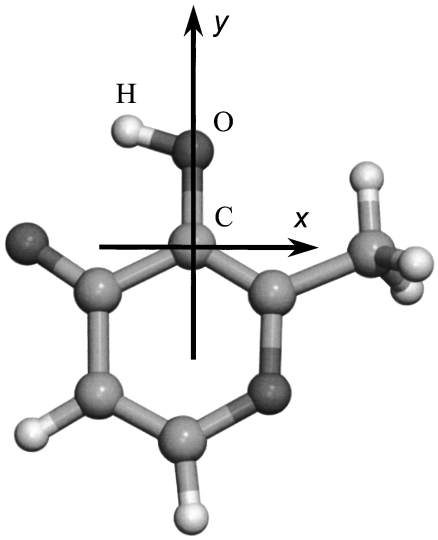

FIG. 1. The lowest energy configuration of 3-hydroxy-2-methyl-4-pyrone and the chosen system of coordinates in *Z*-matrix orientation.

by correctly incorporating those internal coordinates corresponding to the vibrational distortions of interest, it is possible to significantly reduce the dimension of the dynamical model and still achieve a good description of the processes.[21] The potential energy surface (PES) describing vibrational motion of the alcohol hydrogen is expanded in two dimensions in this work. It is even possible, as we show in following sections, to introduce an indirect interdependence among all the internal coordinates of the molecule when a subset of the internal coordinates for a vibrational mode of interest cannot be easily selected; the interdependence of the internal coordinates is contained within terms of the *G*-matrix which appears in the kinetic energy operator.[22] However, complicated expressions for the kinetic energy operator arise since

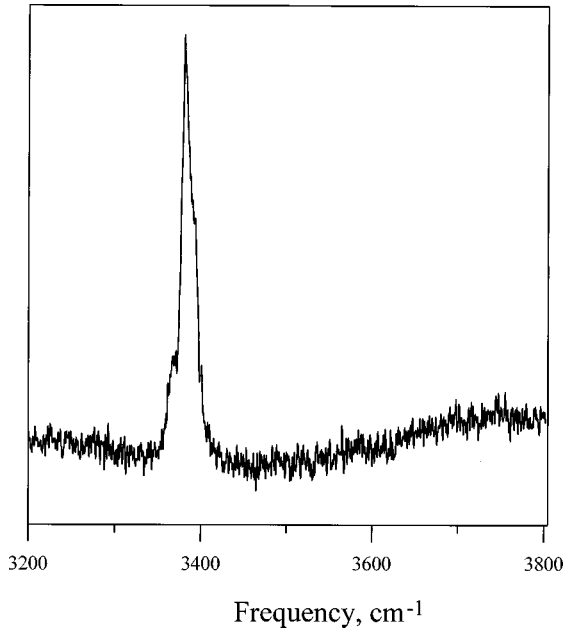

FIG. 2. The part of the IR matrix isolation spectrum corresponding to the O-H stretching band.

internal coordinates often happen to be curvilinear.[23,24] The following section outlines the procedure used to find the functional dependence of *G*-matrix elements on the coordinates describing the O-H stretch. As it is demonstrated in this work, the combination of the accurate kinetic energy terms and an accounting of the anharmonic features of the potential energy surface allowed us to reproduce the experimentally observed O-H stretching frequency for 3-hydroxy-2-methyl-4-pyrone.

II. *G*-MATRIX METHOD FOR VIBRATIONAL FREQUENCY CALCULATIONS

A. Traditional approach

The theoretical study of molecular vibrations stems from the fundamental work of Wilson *et al.*[22] In their treatment, the internal coordinates $\mathbf{s}=(s_1,\ldots,s_{3N-6})$ of an N atom molecule have a linear relationship to the Cartesian coordinates $(\mathbf{r}_1,\ldots,\mathbf{r}_N)=(x_1,\ldots,x_{3N})$,

$$d\mathbf{s}=\mathbf{B}d\mathbf{x}. \tag{1}$$

$\mathbf{B}$ is a $3N-6$ by $3N$ matrix with elements given by $\mathbf{B}_{ij}=(ds_i/dx_j)$. For small amplitude vibrations, the classical kinetic energy can be written as

$$T=\frac{1}{2}\tilde{\dot{\mathbf{x}}}\cdot\mathbf{M}\cdot\dot{\mathbf{x}}=\frac{1}{2}\tilde{\dot{\mathbf{s}}}\cdot\tilde{\mathbf{B}}^{-1}\cdot\mathbf{M}\cdot\mathbf{B}^{-1}\cdot\dot{\mathbf{s}}=\frac{1}{2}\tilde{\dot{\mathbf{s}}}\cdot\mathbf{G}^{-1}\cdot\dot{\mathbf{s}}, \tag{2}$$

where $\mathbf{M}$ is a diagonal $3N$ by $3N$ matrix whose elements are the atomic masses, and

$$\mathbf{G}^{-1}=\tilde{\mathbf{B}}^{-1}\cdot\mathbf{M}\cdot\mathbf{B}^{-1},\quad\text{or}\quad\mathbf{G}=\mathbf{B}\cdot\mathbf{M}^{-1}\cdot\tilde{\mathbf{B}} \tag{3}$$

are the $3N-6$ by $3N-6$ matrices introduced by Wilson. With the use of internal coordinates, which are a natural choice in a description of the intermolecular motion, the potential energy, $V(\mathbf{s})$, of the system can be readily written in a compact form even in those cases where multiple minima appear in the potential hypersurface. The resulting expression of the classical rovibrational Hamiltonian for the system becomes

$$H(\mathbf{p},\mathbf{s})=\frac{1}{2}\tilde{\mathbf{p}}\cdot\mathbf{G}\cdot\mathbf{p}+V(\mathbf{s}), \tag{4}$$

where the elements of the vector $\mathbf{p}$ are the momenta conjugate to the internal coordinates $\mathbf{s}$.

In the quantum mechanical case, however, the kinetic energy operator in internal coordinates takes a much more complicated form.[23] The Hamiltonian operator representing the nuclear motion of an N atom molecule in Cartesian coordinates is given by

$$H=\sum_{\alpha=1}^{N}\frac{1}{2m_\alpha}\nabla_\alpha^2+V. \tag{5}$$

The squared momentum operator within the kinetic energy expression is represented by Laplacian, $\nabla_\alpha^2\equiv[(\partial^2/\partial x_{3\alpha-2}^2)+(\partial^2/\partial x_{3\alpha-1}^2)+(\partial^2/\partial x_{3\alpha}^2)]$. Separation of the translational degrees of freedom and transformation of Laplacian from the Cartesian coordinates to a general set of internal coordinates forces the Hamiltonian to take the form[23]

$$H=-\frac{1}{2}|g|^{-1/2}\sum_{i=1}^{3N-6}\frac{\partial}{\partial s_i}\left(|g|^{1/2}\sum_{j=1}^{3N-6}g^{ij}\frac{\partial}{\partial s_j}\right)+V. \quad (6)$$

In the above expression $|g|$ is the determinant of a matrix whose elements are defined as

$$g_{ij}=\sum_{\alpha=1}^{N}m_\alpha\frac{\partial \mathbf{r}_\alpha}{\partial s_i}\frac{\partial \mathbf{r}_\alpha}{\partial s_j}, \quad (7)$$

and $|g|^{1/2}$ is the Jacobian of the Cartesian coordinates with respect to the $\{s_i\}$ coordinates. The corresponding contravariant components of g^{ij}, which enter the expression (5) for the Hamiltonian, are defined as

$$g^{ij}=\sum_{\alpha=1}^{N}\frac{1}{m_\alpha}\frac{\partial s_i}{\partial \mathbf{r}_\alpha}\frac{\partial s_j}{\partial \mathbf{r}_\alpha}. \quad (8)$$

It is possible to rewrite Eq. (5) as

$$H=-\frac{1}{2}\sum_{i,j=1}^{3N-6}\left(\frac{\partial}{\partial s_i}+\frac{1}{4}\frac{\partial(\ln|g|)}{\partial s_i}\right)\times g^{ij}\left(\frac{\partial}{\partial s_j}-\frac{1}{4}\frac{\partial(\ln|g|)}{\partial s_j}\right)+V. \quad (9)$$

Assuming that the change of $\ln|g|$ with respect to the change of internal coordinate is much smaller than the similar type of contribution from the individual components g^{ij}, this expression for H can be further reduced to[25]

$$H\simeq-\frac{1}{2}\sum_{i,j=1}^{3N-6}\frac{\partial}{\partial s_i}g^{ij}\frac{\partial}{\partial s_j}+V. \quad (10)$$

Comparing the last expression with Eq. (2) one can see that the covariant tensor g_{ij} is equivalent to the $\mathbf{G}^{-1}$ matrix, and the contravariant tensor g^{ij} is equivalent to the $\mathbf{G}$ matrix. Tabulated (constant) values for g^{ij} are traditionally used to calculate the kinetic part of the Hamiltonian matrix.

B. Present approach

Wilson[22] assumed that, since the vibrational amplitudes are usually ''small,'' then the elements g_{ij} must be constant. However, as it follows from Eq. (7), this approximation can not be accurate for those cases when the positions of the atoms close to the group of atoms directly involved in the particular vibration are affected. An example of such situations is the O-H vibration in organic acids which, when excited to higher levels, may lead to a proton-transfer process which usually results in substantial changes in the distances of the nearby bonds. The functional form of the g_{ij} elements can be found by determining the value of the g-matrix for a variety of molecular configurations at different locations on the potential energy surface. In the present work, we consider the motion of the alcohol hydrogen in the plane of the molecule, thus our internal coordinates s_j in Eq. (6) have been chosen to be the x and y coordinates of the hydrogen atom defined in such a way that C-O bond was aligned with the y axis, and the center of the coordinate system was placed at the carbon atom as shown on Fig. 1. The potential energy surface was obtained by incrementally changing the values of x and y and optimizing all the other coordinates. The individual elements g^{ij} for every molecular configuration were calculated directly from Eq. (7) in the following way: for every point (x_μ,y_ν) on the grid, each of the internal coordinates, x and y, was changed by ± 0.01 Å. The geometry of each of the resulting four configurations, ($x_\mu \pm 0.01$ Å, $y_\nu \pm 0.01$ Å), as well as the geometry of the point (x_μ,y_ν) were expressed in the center-of-mass Cartesian coordinate system. Next, each of the geometries was rotated in such a way that the Eckart conditions,[26]

$$\sum_{\alpha=1}^{N}m_\alpha(\mathbf{r}_\alpha^{(e)}+\mathbf{d}_\alpha)=0, \quad (11)$$

$$\sum_{\alpha=1}^{N}m_\alpha(\mathbf{r}_\alpha^{(e)}\times\mathbf{d}_\alpha)=0 \quad (12)$$

were satisfied with respect to the global minimum structure (equilibrium configuration) represented in the center-of-mass coordinate system. $\mathbf{r}_\alpha^{(e)}$ indicates the position vector of the αth atom in the equilibrium structure, and $\mathbf{d}_\alpha$ represents the displacement from the equilibrium position for each particular conformation. By enforcing the Eckart conditions the overall rotation of the molecule is effectively decoupled from the vibrational motion.[26] Four geometries obtained in this way, along with the geometry of the original unshifted configuration, were used to determine the functional dependence of all the Cartesian coordinates with respect to the change of *internal* coordinates x and y at the (x_μ,y_ν) point. Namely, the set of the five values $\{Z(x_\mu,\ y_\nu),\ Z(x_\mu,\ y_\nu+0.01$ Å, $Z(x_\mu,y_\nu-0.01$ Å), $Z(x_\mu+0.01$ Å, $y_\nu)$, $Z(x_\mu-0.01$ Å, $y_\nu)\}$ of a particular Cartesian coordinate Z was approximated by a two-dimensional quadratic polynomial $\mathcal{Z}(x,y)=c_1+c_2\cdot x+c_3\cdot y+c_4\cdot x^2+c_5\cdot y^2$. Then the partial derivatives $\partial\mathcal{Z}(x,y)/\partial x$ and $\partial\mathcal{Z}(x,y)/\partial y$ were calculated at the point (x_μ,y_ν) and inserted into Eq. (7). Next, the calculated matrix $g_{ij}(x_\mu,y_\nu)$ was inverted to give the sought values g^{ij} for the considered grid point (x_μ,y_ν). The values of g^{ij} were calculated for each of the points on the potential energy surface and fitted by a series of two-dimensional shifted Gaussian functions,

$$g^{ij}(x,y)=C_{0ij}+\sum_{m=1}^{M_{g^{ij}}}C_{mij}\cdot e^{-\beta_{mij}^{(x)}(x-x_{mij}^{(g)})^2}\cdot e^{-\beta_{mij}^{(y)}(y-y_{mij}^{(g)})^2}=\sum_{m=0}^{M_{g^{ij}}}C_{mij}\cdot e^{-\beta_{mij}^{(x)}(x-x_{mij}^{(g)})^2}\cdot e^{-\beta_{mij}^{(y)}(y-y_{mij}^{(g)})^2},$$

$$\beta_{0ij}^{(x)}=\beta_{0ij}^{(x)}=0. \quad (13)$$

Such coordinate dependence of the g^{ij} values complicates the kinetic energy term in the Hamiltonian, but makes it possible for more accurate calculations of the vibrational frequencies. The basis set of two-dimensional shifted Gaussian functions combined with polynomials,

$$\{\Psi_\mu(x,y)\}_{\mu=1}^{M_b\times M_b}\equiv\{\varphi_i(x)\cdot\varphi_j(y)\}_{i,j=1}^{M_b}=\{(x-x_i)^{n_i^{(x)}}e^{(-\alpha_i^{(x)}(x-x_i)^2)}\cdot(y-y_i)^{n_j^{(y)}}e^{(-\alpha_j^{(y)}(y-y_i)^2)}\}_{i,j=1}^{M_b}, \quad (14)$$

was employed to solve the vibrational problem. An analytic expression for kinetic energy matrix elements in this basis set has been derived and assumed this form (which, unfortunately, cannot be further simplified),

$$\langle\Psi_\mu|-\frac{1}{2}\frac{d}{dx}g^{11}(x,y)\frac{d}{dx}-\frac{1}{2}\frac{d}{dx}g^{12}(x,y)\frac{d}{dy}-\frac{1}{2}\frac{d}{dy}g^{21}(x,y)\frac{d}{dx}-\frac{1}{2}\frac{d}{dy}g^{22}(x,y)\frac{d}{dy}|\Psi_\nu\rangle$$

$$\equiv\langle\varphi_i(x)\varphi_j(y)|-\frac{1}{2}\frac{d}{dx}g^{11}(x,y)\frac{d}{dx}-\frac{1}{2}\frac{d}{dx}g^{12}(x,y)\frac{d}{dy}-\frac{1}{2}\frac{d}{dy}g^{21}(x,y)\frac{d}{dx}-\frac{1}{2}\frac{d}{dy}g^{22}(x,y)\frac{d}{dy}|\varphi_k(x)\varphi_l(y)\rangle$$

$$=-\frac{1}{2}\sum_{m=0}^{M_{g^{11}}}C_{m11}\cdot\Bigg\{(-2\beta_{m11}^{(x)})\cdot P^{n_j^{(y)},n_l^{(y)}}_{\alpha_j^{(y)},\beta_{m11}^{(y)},\alpha_l^{(y)},y_j,y_{m11}^{(g)},y_l}\cdot\Bigg[(n_k^{(x)}-1)\cdot n_k^{(x)}\cdot P^{n_i^{(x)},n_k^{(x)}-2}_{\alpha_i^{(x)},\beta_{m11}^{(x)},\alpha_k^{(x)},x_i,x_{m11}^{(g)},x_k}-2\alpha_k^{(x)}\cdot n_k^{(x)}$$

$$\cdot P^{n_i^{(x)},n_k^{(x)}-2}_{\alpha_i^{(x)},\beta_{m11}^{(x)},\alpha_k^{(x)},x_i,x_{m11}^{(g)},x_k}-2\alpha_k^{(x)}\cdot(n_k^{(x)}+1)\cdot P^{n_i^{(x)},n_k^{(x)}}_{\alpha_i^{(x)},\beta_{m11}^{(x)},\alpha_k^{(x)},x_i,x_{m11}^{(g)},x_k}+4\cdot(\alpha_k^{(x)})^2\cdot P^{n_i^{(x)},n_k^{(x)}+2}_{\alpha_i^{(x)},\beta_{m11}^{(x)},\alpha_k^{(x)},x_i,x_{m11}^{(g)},x_k}\Bigg]\Bigg\}$$

$$-\frac{1}{2}\sum_{m=0}^{M_{g^{12}}}C_{m12}\cdot\Bigg\{(-2\beta_{m12}^{(x)})\cdot P^{n_i^{(x)},1,n_l^{(x)}}_{\alpha_i^{(x)},\beta_{m12}^{(x)},\alpha_k^{(x)},x_i,x_{m12}^{(g)},x_l}\cdot\Bigg[n_l^{(y)}\cdot P^{n_j^{(y)},n_l^{(y)}-1}_{\alpha_j^{(y)},\beta_{m12}^{(y)},\alpha_l^{(y)},y_j,y_{m12}^{(g)},y_l}-2\alpha_l^{(y)}\cdot P^{n_j^{(y)},n_l^{(y)}+1}_{\alpha_j^{(y)},\beta_{m12}^{(y)},\alpha_l^{(y)},y_j,y_{m12}^{(g)},y_l}\Bigg]$$

$$+\Bigg[n_k^{(x)}\cdot P^{n_i^{(x)},n_k^{(x)}-1}_{\alpha_i^{(x)},\beta_{m12}^{(x)},\alpha_k^{(x)},x_i,x_{m12}^{(g)},x_k}-2\alpha_k^{(x)}\cdot P^{n_i^{(x)},n_k^{(x)}+1}_{\alpha_i^{(x)},\beta_{m12}^{(x)},\alpha_k^{(x)},x_i,x_{m12}^{(g)},x_k}\Bigg]\cdot\Bigg[n_l^{(y)}\cdot P^{n_j^{(y)},n_l^{(y)}-1}_{\alpha_j^{(y)},\beta_{m12}^{(y)},\alpha_l^{(y)},y_j,y_{m12}^{(g)},y_l}-2\alpha_l^{(y)}$$

$$\cdot P^{n_j^{(y)},n_l^{(y)}+1}_{\alpha_j^{(y)},\beta_{m12}^{(y)},\alpha_l^{(y)},y_j,y_{m12}^{(g)},y_l}\Bigg]-\frac{1}{2}\sum_{m=0}^{M_{g^{21}}}C_{m21}\cdot\Bigg\{(-2\beta_{m21}^{(y)})\cdot P^{n_j^{(y)},1,n_l^{(y)}}_{\alpha_j^{(y)},\beta_{m21}^{(y)},\alpha_l^{(y)},y_j,y_{m21}^{(g)},y_l}\cdot\Bigg[n_k^{(x)}\cdot P^{n_i^{(x)},n_k^{(x)}-1}_{\alpha_i^{(x)},\beta_{m21}^{(x)},\alpha_k^{(x)},x_i,x_{m21}^{(g)},x_k}$$

$$-2\alpha_k^{(x)}\cdot P^{n_i^{(x)},n_k^{(x)}+1}_{\alpha_i^{(x)},\beta_{m21}^{(x)},\alpha_k^{(x)},x_i,x_{m21}^{(g)},x_k}\Bigg]\Bigg\}+\Bigg[n_k^{(x)}\cdot P^{n_i^{(x)},n_k^{(x)}-1}_{\alpha_i^{(x)},\beta_{m21}^{(x)},\alpha_k^{(x)},x_i,x_{m21}^{(g)},x_k}-2\alpha_k^{(x)}\cdot P^{n_i^{(x)},n_k^{(x)}+1}_{\alpha_i^{(x)},\beta_{m21}^{(x)},\alpha_k^{(x)},x_i,x_{m21}^{(g)},x_k}\Bigg]$$

$$\cdot\Bigg[n_l^{(y)}\cdot P^{n_j^{(y)},n_l^{(y)}-1}_{\alpha_j^{(y)},\beta_{m21}^{(y)},\alpha_l^{(y)},y_j,y_{m21}^{(g)},y_l}-2\alpha_l^{(y)}\cdot P^{n_j^{(y)},n_l^{(y)}+1}_{\alpha_j^{(y)},\beta_{m21}^{(y)},\alpha_l^{(y)},y_j,y_{m21}^{(g)},y_l}\Bigg]-\frac{1}{2}\sum_{m=0}^{M_{g^{22}}}C_{m22}\cdot\Bigg\{(-2\beta_{m22}^{(y)})\cdot P^{n_i^{(x)},n_k^{(x)}}_{\alpha_i^{(x)},\beta_{m22}^{(x)},\alpha_k^{(x)},x_i,x_{m22}^{(g)},x_k}$$

$$\cdot\Bigg[n_l^{(y)}\cdot P^{n_j^{(y)},1,n_l^{(y)}-1}_{\alpha_j^{(y)},\beta_{m22}^{(y)},\alpha_l^{(y)},y_j,y_{m22}^{(g)},y_l}-2\alpha_l^{(y)}\cdot P^{n_j^{(y)},1,n_l^{(y)}+1}_{\alpha_j^{(y)},\beta_{m22}^{(y)},\alpha_l^{(y)},y_j,y_{m22}^{(g)},y_l}\Bigg]+P^{n_i^{(x)},n_k^{(x)}}_{\alpha_i^{(x)},\beta_{m22}^{(x)},\alpha_k^{(x)},x_i,x_{m22}^{(g)},x_k}$$

$$\cdot\Bigg[(n_l^{(y)}-1)\cdot n_l^{(y)}\cdot P^{n_j^{(y)},n_l^{(y)}-2}_{\alpha_j^{(y)},\beta_{m22}^{(y)},\alpha_l^{(y)},y_j,y_{m22}^{(g)},y_l}-2\alpha_l^{(y)}\cdot n_l^{(y)}\cdot P^{n_j^{(y)},n_l^{(y)}}_{\alpha_j^{(y)},\beta_{m22}^{(y)},\alpha_l^{(y)},y_j,y_{m22}^{(g)},y_l}-2\alpha_l^{(y)}\cdot(n_l^{(y)}+1)$$

$$\cdot P^{n_j^{(y)},n_l^{(y)}}_{\alpha_j^{(y)},\beta_{m22}^{(y)},\alpha_l^{(y)},y_j,y_{m22}^{(g)},y_l}+4\cdot(\alpha_l^{(y)})^2\cdot P^{n_j^{(y)},n_l^{(y)}+2}_{\alpha_j^{(y)},\beta_{m22}^{(y)},\alpha_l^{(y)},y_j,y_{m22}^{(g)},y_l}\Bigg]\Bigg\},$$

where the 8-P and 9-P symbols are described in the Appendix.

The potential energy curve in our method is fitted by the following series of functions,

$$V(x,y)=\sum_{m=0}^{M_V}a_m\cdot e^{-\gamma_m^{(x)}(x-x_m^{(V)})^2}\cdot e^{-\gamma_m^{(y)}(y-y_m^{(V)})^2}. \tag{15}$$

The functions used in the expansion (15) ensure the correct behavior at infinity, as well as reproduce all the local significant features of the potential near the minima. Such expansion results in the following form of the potential energy matrix elements,

$$\langle\Psi_\mu|V(x,y)|\Psi_\nu\rangle\equiv\langle\varphi_i(x)\varphi_j(y)|V(x,y)|\varphi_k(x)\varphi_l(y)\rangle$$

$$=\sum_{m=0}^{M_V}a_l\cdot P^{n_i^{(x)},n_k^{(x)}}_{\alpha_i^{(x)},\gamma_m^{(x)},\alpha_k^{(x)},x_i,x_m^{(V)},x_k}\cdot P^{n_j^{(y)},n_l^{(y)}}_{\alpha_j^{(y)},\gamma_l^{(y)},\alpha_m^{(y)},y_j,y_m^{(V)},y_l}, \tag{16}$$

expressed with help of 8-P and 9-P symbols (see the Appendix).

Finally, values of the overlap matrix for the employed basis set (14) are given by

$$\langle\Psi_\mu|\Psi_\nu\rangle\equiv\langle\phi_i(x)|\phi_k(x)\rangle\cdot\langle\phi_j(y)|\phi_l(y)\rangle$$

$$=P^{n_i^{(x)},n_k^{(x)}}_{\alpha_i^{(x)},\alpha_k^{(x)},0,x_i,x_k,0}\cdot P^{n_j^{(y)},n_l^{(y)}}_{\alpha_j^{(y)},\alpha_m^{(y)},0,y_j,y_l,0}. \tag{17}$$

Knowing the explicit form of all the necessary matrix elements, the matrix equation for the vibrational problem,

$$HC=ESC, \tag{18}$$

can be solved.

III. CALCULATIONS AND RESULTS

A. Geometry optimizations

The potential energy surface was calculated using the GAUSSIAN 92[27] and GAUSSIAN 94[28] programs. The molecule's geometry was optimized at the SCF/3-21G level and then calculations of single point energies at the MP2/6-31+G** level of theory were performed utilizing the self-consistent

field (SCF) geometries. The 6-31+G** basis includes diffused orbitals (+) and polarization functions (**) and should describe the hydrogen bond reasonably well.

In the first optimization we determined the 3-hydroxy-2-methyl-4-pyrone geometry at the global minimum, which corresponds to the configuration with the proton near the alcohol oxygen. Next, the geometry optimization with the proton at the ketone oxygen was carried by placing the proton nearer to the ketone oxygen. Over 100 more geometry optimizations were performed in order to provide sufficient data for the potential energy surface. The calculations were done by varying the O-H bond length and C-O-H bond angle (see Fig. 1), while allowing the rest of the molecule's coordinates to relax. The bond length was varied from 0.8 to 2.15 Å in increments of 0.05 Å, and the bond angle was varied from 75 to 140 deg in increments of 5 deg.

B. Potential energy surface (PES) calculations

The majority of the MP2 calculations were carried out with the proton near to the global minimum, since this portion of the potential surface is the most important in the vibrational calculations which followed. It was found that the PES has two minima: a global minimum with the hydrogen atom at the alcohol oxygen, and a local minimum with the proton on the ketone oxygen. At the MP2/6-31+G** level, the energy at the global minimum was −456.628 303 hartrees, and the energy at the local minimum was −456.611 299 hartrees. The difference in energy of these two minima was 0.0170 hartrees (3731 cm^{-1}). The barrier between the two minima is approximately −456.6038 hartrees, which is 5487 cm^{-1} above the global minimum and 1646 cm^{-1} above the local minimum.

The shape of the potential energy surface at the global minimum reflects the anharmonicity of the motion of the proton from its equilibrium position. The PES is more trough shaped than quadratic, due to the proton's interaction with the ketone oxygen. If there were no hydrogen bonding, this minimum would be more quadratic. The local minimum is significantly more quadratic than the global (see Fig. 3).

C. Surface fit to the PES

The coordinates and energy corresponding to the global minimum were subtracted from all data points, which enabled us to place a half of the basis functions at the origin for the variational calculations. We chose a set of two-dimensional Gaussian functions (14) to represent the potential surface. Gaussian functions were used because they could accurately describe the two minima, the barrier between them, as well as the correct asymptotic behavior. We also placed emphasis on the points about the minima of the surface with weighing factors. The functional fit to the PES was made using ten fully optimized Gaussian functions of type (14). Fitting involved a simultaneous optimization of 50 parameters (10 linear and 40 nonlinear ones) which appeared to be quite a formidable task. The optimization was performed via an iterative procedure consisting of an exact solution for the linear coefficients using a singular value decomposition routine with a fixed set of nonlinear parameters

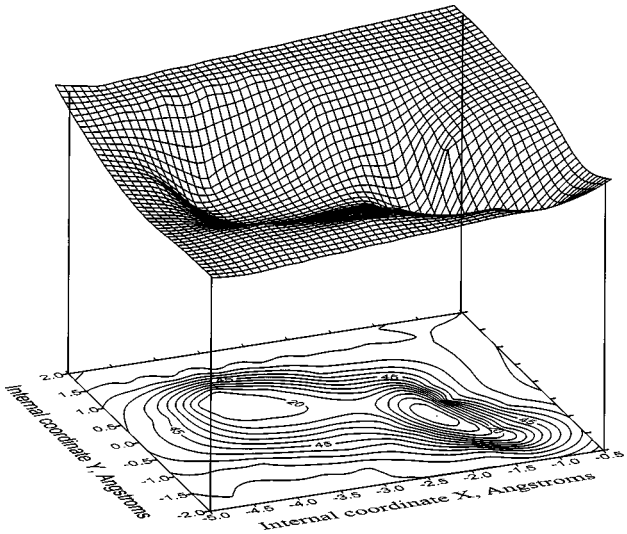

FIG. 3. The potential energy surface of 3-hydroxy-2-methyl-4-pyrone calculated at MP2/6-31+G** level of theory (the numbers on the contour plot are reported in mhartrees).

determined by a quasi-Newton gradient search method in each iteration. It was found that sufficiently high-order polynomial fits can also reproduce calculated PES values with similar accuracy, but incorrect asymptotic behavior, as well as the wiggling in between the data points (especially for higher order polynomials), would necessarily influence the values of the potential energy matrix elements and, hence, the resulted frequencies.

D. Calculations of the contravariant g^{ij} components

It was found that the g^{ij}-values do not stay constant but, rather, vary as a function of the internal coordinates x and y (see Figs. 4, 5, and 6). As one can see from the figures, the increase and decrease of the g-values coincide with the

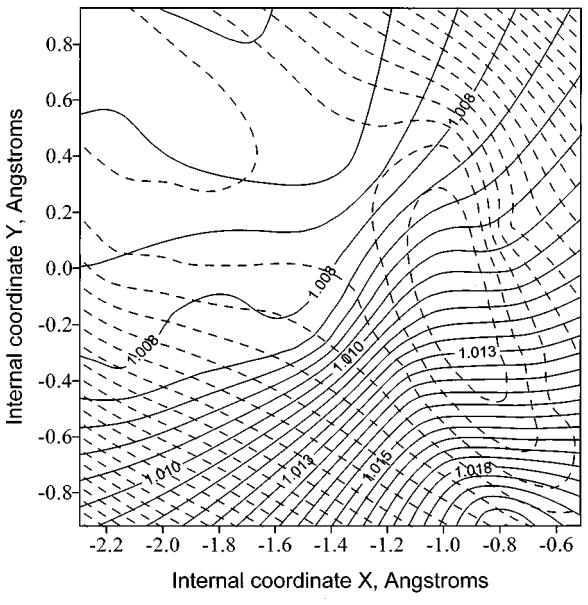

FIG. 4. Contour plot of $g^{11}(x,y)$ component in amu (solid lines) vs projection of PES onto x-y plane (dashed lines).

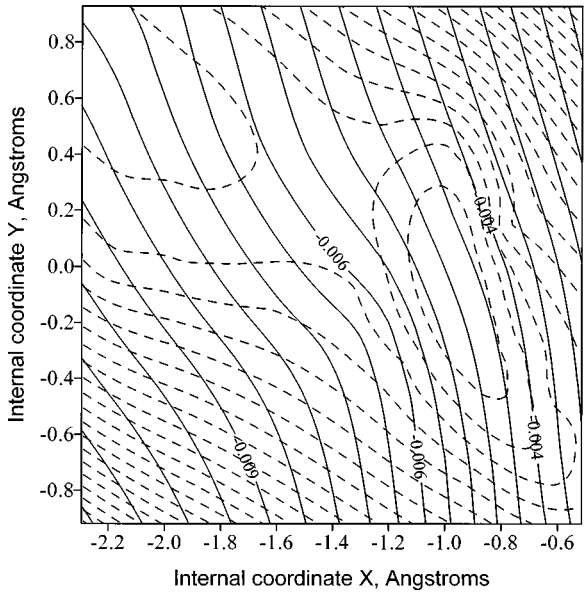

FIG. 5. Contour plot of $g^{12}(x,y)$ component in amu (solid lines) vs projection of PES onto x-y plane (dashed lines).

change in the potential energy as the hydrogen travels across the barrier (see Figs. 4, 5, and 6). The observed situation agrees with the theory discussed earlier, i.e., as it follows from definition of g, Eq. (7), the contribution to the value of the effective mass must be sensitive to the change of the positions of *all* atoms in the molecule. The functional dependence of the g-values played a significant role in obtaining more accurate results compared to those from the constant-g method. Each individual g-component was fitted by the series of functions of the form (13). It was found that the results for the variable g-matrix approach better agree with the experiment than the values obtained using constant g^{ij}-values calculated as an average over the studied grid region. Eight fully optimized functions in the expansion (13)

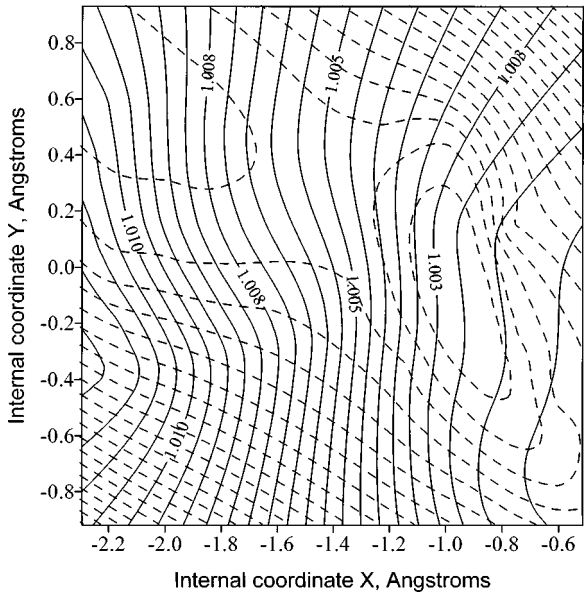

FIG. 6. Contour plot of $g^{22}(x,y)$ component in amu (solid lines) vs projection of PES onto x-y plane (dashed lines).

TABLE I. O-H stretching frequency of 3-hydroxy-2-methyl-4-pyrone obtained using different methods.

Method	ν_{stretch} (cm^{-1})
Harmonic[a] MP2/6-31+G**	3291.10
Variable-g using 6-point harmonic fit	3489.14
Constant-g method	3414.43
Variable-g not including cross terms	**3398.97**
Variable-g including cross terms	**3393.41**
Experiment[b]	3381

[a]Results from GAUSSIAN 94 obtained at the MP2/6-31+G** level of theory using analytic second derivatives and the geometry reoptimized at the same level.
[b]Frequencies measured in IR low-temperature matrix isolation experiment.

were enough to reach the required accuracy (standard deviation) $\sigma^2=10^{-4}$ for both g^{11} and g^{22} fits. The contributions from the cross terms g^{12} and g^{21} (which must be equal due to the Hermitian properties of the kinetic energy operator) to the corresponding matrix elements, as well as to the resulting frequencies, were found to be rather small (about 0.1%). The inclusion of these terms reduced the discrepancies between the calculated and experimental values by about 5 cm^{-1} (see Table I). Since the g^{12} and g^{21} components were not changing much and happened to be small relative to g^{11} and g^{22} values (see Fig. 4), we assumed the cross terms to be constants in our calculations and put them equal to the average g^{12} value.

E. Frequency calculations

The intramolecular hydrogen bond in 3-hydroxy-2-methyl-4-pyrone causes the O-H vibration to be anharmonic (see Fig. 3). The functional fit to the PES was used in the vibrational Hamiltonian, and the reduced-dimension Schrödinger equation for the nuclear motion of the proton was variationally solved for the expectation values. The exponents $\alpha_i^{(x)}=\alpha^{(x)}$ and $\alpha_j^{(y)}=\alpha^{(y)}$ in Eq. (14) were found from the harmonic approximation, and then the functional basis was expanded by including functions with powers of the preexponential polynomials $n_i^{(x)}$ and $n_j^{(y)}$ ranging from 0 to M_b-1. The polynomial part ensured that the eigenfunctions for the vibrational problem could be flexible enough to be oriented in any direction on the potential surface, thus providing an accurate tool for description of the vibrational dynamics. Half of the basis functions were chosen to be centered at the first minimum and the other half at the second one. This choice allowed us to account for the possibility of the moving hydrogen to appear at both minima on the potential surface. We also did a comparative study on different choices of the basis set. We examined a basis with fewer preexponential power factors but with several different exponential components [$\alpha_i^{(x)}=2^n\alpha^{(x)}$, $\alpha_j^{(y)}=2^n\alpha^{(y)}$, $n=\pm1$, ±2]. The results indicate that increasing the range of powers $n_i^{(x)}$ and $n_j^{(y)}$ and having only two α's, $\alpha^{(x)}$ and $\alpha^{(y)}$, in all the basis functions, is the most efficient way to consistently obtain lower eigenvalues.

Once the variational calculation was completed, the energy spectrum was analyzed to identify the vibrational frequencies corresponding to the combined O-H stretching and

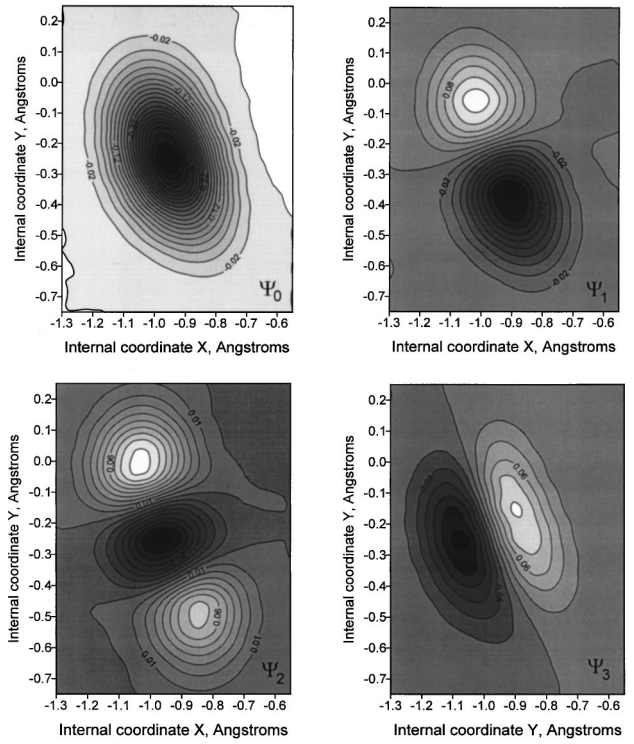

FIG. 7. Contour plots of the wave functions corresponding to the lowest four vibrational eigenvalues.

wagging motions in 3-hydroxy-2-methyl-4-pyrone. The assignment of the lines did not present any difficulties due to a considerable difference in nature of the wave functions corresponding to the stretching and bending modes. One expects to find the nodes for the bending motion to be located along the minimum energy valley between the two minima on the potential energy surface, whereas the nodes for the stretching mode should be located perpendicular to that valley. In Fig. 7 we show the contour plots of the wave functions corresponding to the four lowest vibrational energy eigenvalues. One can clearly see that the wave functions of the first and the fourth states fit the description of the stretching motion. The energy difference between these two levels gives the stretching frequency $\nu_{0\rightarrow 1}$. We found that for the studied vibration the values for the frequencies converge fairly rapidly to the asymptotic values with increase of the number of the basis functions (see Table II).

Accounting for the anharmonicity effects in O-H vibration also played a major role in obtaining accurate results for the frequencies. In fact, the frequencies from our variable-g method, which fully accounts for anharmonicity, were found to be 3393 vs 3381 cm^{-1} (experimental). Although, if one uses just a quadratic two-dimensional six-point fit near the bottom of the first minima, i.e., assumes a harmonic nature of the electronic potential, the results for the vibrational frequencies increase dramatically by about 100 cm^{-1}, even though the accurate kinetic energy expression is employed. The harmonic calculation using GAUSSIAN 94 at the MP2/6-31+G** level of theory (and the geometry reoptimized at the same level) was also performed for comparison. The harmonic frequency, scaled by a factor of 0.9, resulted in a value of 3291 which was 90 cm^{-1} lower than the experimentally observed value. A comparison of experimental and theoretically calculated frequencies are summarized in Table I. From these values one can see very clearly that for complicated situations, i.e., coupled vibrational modes resulting from the presence of the nearby highly electronegative atoms, the major role is played by the coordinate-dependent effective mass tensor corresponding to the coupled modes, although the anharmonic features of the electronic potential should also be considered in order to reproduce the experimental frequencies.

TABLE II. Convergence analysis for the O-H stretching frequencies of 3-hydroxy-2-methyl-4-pyrone obtained by variable-g matrix method.

Dimension of basis	ν_{stretch} from variable-g matrix method with cross terms (cm^{-1})	ν_{stretch} from variable g-matrix method without cross terms (cm^{-1})
36	3410.01	3415.96
81	3395.91	3400.90
100	3394.53	3399.18
400	3393.41	3398.97

IV. CONCLUSION

The O-H stretching vibration in 3-hydroxy-2-methyl-4-pyrone was studied. The MP2/6-31+G** potential energy surface was used in the calculations. A good agreement between experimental and calculated spectra was obtained. The need for the variable g-matrix method becomes especially pronounced when the strong hydrogen bonds are present in the molecule, the situation often encountered in biological systems.

APPENDIX

Analytical formulas for the values entering overlap, potential, and kinetic energy matrices can be very convoluted if the shifted Gaussian functions combined with polynomials are involved as a basis set. Here we give explicit formulas for ''auxiliary'' symbols (we call them P- and Q-symbols) which make the final analytical expressions several times shorter and much easier to program. P-symbols stem from the analytical evaluations of the integrals of the following type:

$$
\begin{aligned}
&P^{(n)}_{\alpha_1,\alpha_2,\alpha_3,x_1,x_2,x_3} \\
&\quad\equiv \int_{-\infty}^{\infty} e^{-\alpha_1(x-x_1)^2}\cdot e^{-\alpha_2(x-x_2)^2}\cdot e^{-\alpha_3(x-x_3)^2}\cdot x^n dx \\
&\quad= e^{-(\alpha_1 x_1^2+\alpha_2 x_2^2+\alpha_3 x_3^2)}\cdot e^{-(\alpha_1 x_1+\alpha_2 x_2+\alpha_3 x_3)^2/(\alpha_1+\alpha_2+\alpha_3)} \\
&\qquad\cdot\left(\frac{1}{2\sqrt{\alpha_1+\alpha_2+\alpha_3}}\right)^{n+1}\cdot\sum_{l=0}^{n}(-1)^l\binom{n}{l} \\
&\qquad\cdot\left(\frac{\alpha_1 x_1+\alpha_2 x_2+\alpha_3 x_3}{2\sqrt{\alpha_1+\alpha_2+\alpha_3}}\right)^{l}\cdot(1+(-1)^{n-l}) \\
&\qquad\cdot\frac{1}{2}\Gamma\left(\frac{n-l+1}{2}\right),
\end{aligned}
\tag{A1}
$$

which we call 7-P symbol. Here $\Gamma(x)$ is the usual gamma function. 8-P and 9-P symbols are evaluated with help of 7-P symbols as

$$P^{n_1,n_2}_{\alpha_1,\alpha_2,\alpha_3,x_1,x_2,x_3} \equiv \int_{-\infty}^{\infty} e^{-\alpha_1(x-x_1)^2}\cdot e^{-\alpha_2(x-x_2)^2}\cdot e^{-\alpha_3(x-x_3)^2}\cdot (x-x_1)^{n_1} \cdot (x-x_2)^{n_2}dx = \sum_{r=0}^{n_1}\sum_{s=0}^{n_2} (-1)^{r+s}\binom{n_1}{r}\binom{n_2}{s} \cdot (x_1)^r (x_2)^s \cdot P^{(n_1+n_2-r-s)}_{\alpha_1,\alpha_2,\alpha_3,x_1,x_2,x_3} \tag{A2}$$

and

$$P^{n_1,n_2,n_3}_{\alpha_1,\alpha_2,\alpha_3,x_1,x_2,x_3} \equiv \int_{-\infty}^{\infty} e^{-\alpha_1(x-x_1)^2}\cdot e^{-\alpha_2(x-x_2)^2}\cdot e^{-\alpha_2(x-x_2)^2}\cdot (x-x_1)^{n_1} \cdot (x-x_2)^{n_2}\cdot (x-x_3)^{n_3}dx = \sum_{r=0}^{n_1}\sum_{s=0}^{n_2}\sum_{t=0}^{n_3} (-1)^{r+s+t} \times \binom{n_1}{r}\binom{n_2}{s}\binom{n_3}{t}\cdot (x_1)^r (x_2)^s (x_3)^t \cdot P^{(n_1+n_2-r-s)}_{\alpha_1,\alpha_2,\alpha_3,x_1,x_2,x_3}, \tag{A3}$$

respectively.

For evaluation of the potential energy matrix, the Morse functions proved to be extremely useful for approximating the behavior of the potential surface corresponding to short bond distances. Here we introduce Q-symbols which are very similar to the P-symbols, but result from the integrals involving parts of the Morse potential. We have, respectively, for the 7-Q and 8-Q symbols,

$$Q^{(n)}_{\alpha_1,\beta,\alpha_2 x_1,x_0,x_2} \equiv \int_{-\infty}^{\infty} e^{-\alpha_1(x-x_1)^2}\cdot e^{-\beta(x-x_0)}\cdot e^{-\alpha_2(x-x_2)^2}\cdot x^n dx = e^{-(\alpha_1 x_1^2+\alpha_2 x_2^2-\beta x_0)}\cdot e^{-(\beta-2\alpha_1 x_1+2\alpha_2 x_2)^2/4(\alpha_1+\alpha_2)} \cdot \left(\frac{1}{\sqrt{\alpha_1+\alpha_2}}\right)^{n+1}\cdot \sum_{l=0}^{n}(-1)^l\binom{n}{l} \cdot \left(\frac{\beta-2\alpha_1 x_1+2\alpha_2 x_2}{2\sqrt{\alpha_1+\alpha_2}}\right)^l \cdot (1+(-1)^{n-l}) \cdot \frac{1}{2}\Gamma\left(\frac{n-l+1}{2}\right), \tag{A4}$$

and

$$Q^{n_1,n_2}_{\alpha_1,\beta,\alpha_2,x_1,x_0,x_2} \equiv \int_{-\infty}^{\infty} e^{-\alpha_1(x-x_1)^2}\cdot e^{-\beta(x-x_0)} \cdot e^{-\alpha_2(x-x_2)^2}(x-x_1)^{n_1}\cdot (x-x_2)^{n_2}dx = \sum_{r=0}^{n_1}\sum_{s=0}^{n_2}(-1)^{r+s}\binom{n_1}{r}\binom{n_2}{s} \cdot (x_1)^r (x_2)^s \cdot Q^{(n_1+n_2-r-s)}_{\alpha_1,\beta,\alpha_2,x_1,x_0,x_2}. \tag{A5}$$

If one chooses a bond length to be one of the internal coordinates,[11] then the range of integration should be changed from $(-\infty,+\infty)$ to $(0,+\infty)$. This introduces the incomplete gamma function $\gamma(x,a)$ to the above formulas (we call the resulted symbols restricted $\tilde{P}$- and $\tilde{Q}$-symbols),

$$\tilde{P}^{(n)}_{\alpha_1,\alpha_2,\alpha_3,x_1,x_2,x_3} \equiv \int_0^{\infty} e^{-\alpha_1(x-x_1)^2}\cdot e^{-\alpha_2(x-x_2)^2}\cdot e^{-\alpha_3(x-x_3)^2}\cdot x^n dx = e^{-(\alpha_1 x_1^2+\alpha_2 x_2^2+\alpha_3 x_3^2)}\cdot e^{-(\alpha_1 x_1+\alpha_2 x_2+\alpha_3 x_3)^2/(\alpha_1+\alpha_2+\alpha_3)}\cdot \left(\frac{1}{2\sqrt{\alpha_1+\alpha_2+\alpha_3}}\right)^{n+1}\cdot \sum_{l=0}^{n}(-1)^l\binom{n}{l} \cdot \left(\frac{\alpha_1 x_1+\alpha_2 x_2+\alpha_3 x_3}{2\sqrt{\alpha_1+\alpha_2+\alpha_3}}\right)^l \cdot \frac{1}{2}\left[(1+(-1)^{n-l})\cdot\Gamma\left(\frac{n-l+1}{2}\right) - (-1)^{n-l}\gamma\left(\frac{n-l+1}{2},\frac{(\alpha_1 x_1^2+\alpha_2 x_2^2+\alpha_3 x_3^2)^2}{4\cdot(\alpha_1+\alpha_2+\alpha_3)}\right)\right]. \tag{A6}$$

Then 8-$\tilde{P}$ and 9-$\tilde{P}$ symbols are expressed via 7-$\tilde{P}$ symbols in exactly the same way as unrestricted 8-P and 9-P symbols are expressed through 7-P,

$$\tilde{P}^{n_1,n_2}_{\alpha_1,\alpha_2,\alpha_3,x_1,x_2,x_3} \equiv \int_0^\infty e^{-\alpha_1(x-x_1)^2}\cdot e^{-\alpha_2(x-x_2)^2}\cdot e^{-\alpha_3(x-x_3)^2}\cdot (x-x_1)^{n_1} \cdot (x-x_2)^{n_2} dx = \sum_{r=0}^{n_1}\sum_{s=0}^{n_2} (-1)^{r+s}\binom{n_1}{r}\binom{n_2}{s} \cdot (x_1)^r (x_2)^s \cdot \tilde{P}^{(n_1+n_2-r-s)}_{\alpha_1,\alpha_2,\alpha_3,x_1,x_2,x_3} \tag{A7}$$

and

$$\tilde{P}^{n_1,n_2,n_3}_{\alpha_1,\alpha_2,\alpha_3,x_1,x_2,x_3} \equiv \int_0^\infty e^{-\alpha_1(x-x_1)^2}\cdot e^{-\alpha_2(x-x_2)^2}\cdot e^{-\alpha_2(x-x_2)^2}\cdot (x-x_1)^{n_1} \cdot (x-x_2)^{n_2}\cdot (x-x_3)^{n_3} dx = \sum_{r=0}^{n_1}\sum_{s=0}^{n_2}\sum_{t=0}^{n_3} (-1)^{r+s+t}\binom{n_1}{r}\binom{n_2}{s}\binom{n_3}{t} \cdot (x_1)^r \times (x_2)^s (x_3)^t \cdot \tilde{P}^{(n_1+n_2-r-s)}_{\alpha_1,\alpha_2,\alpha_3,x_1,x_2,x_3}. \tag{A8}$$

The same applies for 7-$\tilde{Q}$ and 8-$\tilde{Q}$ symbols,

$$\tilde{Q}^{(n)}_{\alpha_1,\beta,\alpha_2 x_1,x_0,x_2} \equiv \int_0^\infty e^{-\alpha_1(x-x_1)^2}\cdot e^{-\beta(x-x_0)}\cdot e^{-\alpha_2(x-x_2)^2}\cdot x^n dx = e^{-(\alpha_1 x_1^2+\alpha_2 x_2^2-\beta x_0)}\cdot e^{-(\beta-2\alpha_1 x_1+2\alpha_2 x_2)^2/4(\alpha_1+\alpha_2)} \cdot \left(\frac{1}{\sqrt{\alpha_1+\alpha_2}}\right)^{n+1}\cdot \sum_{l=0}^{n}(-1)^l\binom{n}{l}\cdot\left(\frac{\beta-2\alpha_1 x_1+2\alpha_2 x_2}{2\sqrt{\alpha_1+\alpha_2}}\right)^l \cdot \frac{1}{2}\left[(1+(-1)^{n-l})\cdot\Gamma\left(\frac{n-l+1}{2}\right) - (-1)^{n-l}\gamma\left(\frac{n-l+1}{2},\frac{(\beta-2\alpha_1 x_1+2\alpha_2 x_2)^2}{4\cdot(\alpha_1+\alpha_2)}\right)\right] \tag{A9}$$

and

$$\tilde{Q}^{n_1,n_2}_{\alpha_1,\beta,\alpha_2,x_1,x_0,x_2} \equiv \int_0^\infty e^{-\alpha_1(x-x_1)^2}\cdot e^{-\beta(x-x_0)}\cdot e^{-\alpha_2(x-x_2)^2}(x-x_1)^{n_1}\cdot(x-x_2)^{n_2}dx = \sum_{r=0}^{n_1}\sum_{s=0}^{n_2}(-1)^{r+s}\binom{n_1}{r}\binom{n_2}{s}\cdot(x_1)^r(x_2)^s\cdot\tilde{Q}^{(n_1+n_2-r-s)}_{\alpha_1,\beta,\alpha_2,x_1,x_0,x_2}. \tag{A10}$$

[1] L. E. Snyder, J. M. Hollis, R. D. Suenram, F. J. Lovas, L. W. Brown, and D. Buhl, Astrophys. J. **268**, 123 (1983).
[2] I. I. Berulis, G. Winnewisser, V. V. Krasnov, and R. L. Sorochenko, Sov. Astron. Lett. **11**, 251 (1985).
[3] J. A. Pople, R. Krishnan, H. B. Schlegel, D. DeFrees, J. S. Binkley, M. J. Frisch, R. F. Whiteside, R. F. Hout, and W. J. Hehre, Int. J. Quantum Chem. Quantum Chem. Symp. **15**, 269 (1981).
[4] D. J. DeFrees, J. Comput. Chem. **82**, 333 (1985).
[5] B. H. Besler, J. Chem. Phys. **89**, 360 (1988).
[6] C. L. Janssen and H. F. Schaefer, J. Chem. Phys. **95**, 5128 (1991).
[7] J. F. Stanton, J. Chem. Phys. **94**, 404 (1991).
[8] M. Flock and M. Ramek, Int. J. Quantum Chem., Quantum Chem. Symp. **27**, 331 (1993).
[9] M. J. Nowak, A. Les, and L. Adamowicz, Trends Phys. Chem. **4**, 137 (1994).
[10] I. D. Reva, A. M. Plokhotnichenko, S. G. Stepanian, A. Yu. Ivanov, E. D. Radchenko, G. G. Sheina, and Yu. P. Blagoi, Chem. Phys. Lett. **232**, 141 (1995).
[11] V. Alexandrov, L. Adamowicz, and S. Stepanian, Chem. Phys. Lett. (submitted).
[12] B. Hess, J. R. Lawrence, J. Schaad, P. Carsky, and R. Zahradnik, Chem. Rev. **86**, 709 (1986).
[13] T. A. Annan, C. Peppe, and D. G. Tuck, Can. J. Chem. **68**, 1598 (1990).
[14] M. N. Rao, K. L. Omprakash, K. J. Charyulu, A. V. Chandrapal, and M. L. N. Reddy, Acta Cienc. Indica, Chem. **12**, 31 (1986).
[15] C. Gerard and R. P. Hugel, C. R. Seances Acad. Sci., Ser. 1 **295**, 175 (1982).
[16] J. Wei, Yaoxue Xuebao **17**, 549 (1982).
[17] J. Wei, Yaoxue Tongbao **17**, 175 (1982).
[18] S. D. Kushch, E. N. Izakovich, O. S. Roshchupkina, V. M. Nichvoloda, and M. L. Khidekel, Izv. Akad. Nauk SSR, **4**, 900 (1981).
[19] C. Garard and R. P. Hugel, J. Chem. Res., Synop. **9**, (1980).
[20] C. Makni, B. Regaya, M. Aplincourt, and C. Kappenstein, C. R. Hebd. Seances Acad. Sci., Ser. C **280**, 117 (1975).
[21] J. E. Hadder and J. H. Frederick, J. Chem. Phys. **97**, 3500 (1992).
[22] E. B. Wilson, *Molecular Vibrations* (Dover, New York, 1955).
[23] B. Podolsky, Phys. Rev. **32**, 812 (1928).
[24] L. J. Schaad and J. Hu, J. Mol. Struct.: THEOCHEM **185**, 203 (1989).
[25] T. B. Malloy, J. Mol. Spectrosc. **44**, 504 (1972).
[26] C. Eckart, Phys. Rev. **47**, 552 (1935).
[27] M. J. Frisch, G. W. Trucks, M. Head-Gordon, P. M. W. Gill, M. W. Wong, J. B. Foresman, B. G. Johnson, H. B. Schlegel, M. A. Robb, E. S. Replogle, R. Gomperts, J. L. Andres, K. Raghavachari, J. S. Binkley, C. Gonzalez, R. L. Martin, D. J. Fox, D. J. Defrees, J. Baker, J. J. P. Stewart, and J. A. Pople, GAUSSIAN 92, Revision G.2 (Gaussian, Inc., Pittsburgh, PA, 1992).
[28] M. J. Frish, G. W. Trucks, H. B. Schlegel, P. M. W. Gill, B. G. Johnson, M. A. Robb, J. R. Cheeseman, T. Keith, G. A. Peterson, J. A. Montgomery, K. Raghavachari, M. A. Al-Laham, V. G. Zakrewskii, J. V. Ortiz, J. B. Foresman, J. Cioslowski, B. B. Stefanov, A. Nanayakkara, M. Challacombe, C. Y. Peng, P. Y. Ayla, W. Chen, M. W. Wong, J. L. Andres, E. S. Replogle, R. Gomperts, R. L. Martin, D. J. Fox, J. S. Binkley, D. J. Defrees, J. Baker, J. P. Stewart, M. Head-Gordon, C. Gonzalez, and J. A. Pople, GAUSSIAN 94, Revision E.2 (Gaussian Inc., Pittsburgh, PA, 1994).